NANO LETTERS

2007
Vol. 7, No. 5
1264−1269

"Quantum Coaxial Cables" for Solar Energy Harvesting

Yong Zhang,*,† Lin-Wang Wang,‡ and Angelo Mascarenhas†

Materials Science Center, National Renewable Energy Laboratory, 1617 Cole Boulevard, Golden, Colorado 80401, and Computational Research Division, Lawrence Berkeley National Laboratory, Berkeley, California 94720

Received January 22, 2007; Revised Manuscript Received March 13, 2007

ABSTRACT

Type II core–shell nanowires based on III–V and II–VI semiconductors are designed to provide the highly desirable but not readily available feature—efficient charge separation—and concurrently address the different material challenges specific for a few key renewable energy applications: including hydrogen generation via photoelectrochemical water splitting, dye-sensitized solar cells, and conventional solar cells. They also open up new avenues for studying novel physics and material sciences in reduced dimensionality of very unusual quasi-one-dimensional systems. A first-principles density function theory within the local density approximation (LDA) is used for the electronic structure calculation and a valence-force-field method for the strutural relaxation, and emprical corrections to the LDA errors are applied.

In a conventional semiconductor, electrons and holes typically stay in the same region after photoexcitation, which is very desirable for certain applications, light-emitting devices for instance, where a maximized wavefunction overlap of the electron and hole yields a high radiative recombination rate. However, for a number of key renewable energy applications, including hydrogen generation via photoelectrochemical water splitting,[1] dye-sensitized solar cells,[2] and even regular solar cells,[3] the efficient charge separation of the electron and hole after photoexcitation is instead highly preferred, although not readily available in the existing repertory of materials. In this work, "quantum coaxial cables", core−shell semiconductor nanowires with large type II band alignments as microscopic architectural analogues of conventional coaxial cables, are designed to provide this feature, and concurrently a superior electronic conductivity, another critical feature for these devices to reach their ultimate efficiency limits.

A conventional coaxial cable is a two-conductor cable consisting of a central wire conductor symmetrically surrounded by a braided conductor with an insulating spacer in between, as shown in Figure 1a. The braid serves as a return channel for the electric current running in the core or allows "holes" (in the language of semiconductor physics) to flow in the opposite direction. We will show that it is possible to design a core−shell semiconductor nanowire, as shown for example in Figure 1b, such that the electron and hole wavefunctions are naturally confined in the core and shell region, respectively, without even having to introduce a barrier layer (the spacer) in between. Such "quantum coaxial cables", besides their unique ability of inducing efficient charge separation, may remedy major material shortcomings for the above-mentioned applications in solar energy harvesting. Specifically, the proposed core−shell nanowire may (1) offer materials with optimized band structure and much better stability for water splitting, (2) provide replacements for the generally less stable sensitizers—dye molecules—with solid-state sensitizers and also greatly extend the coverage of the solar spectrum, and (3) minimize the radiative recombination loss in the conventional solar cell and cover nearly the whole usable solar spectrum in one single ternary system (e.g., from <0.5 eV to >3.0 eV with GaN−GaP). The flexibility of tailoring the material properties to address the specific challenge of each individual application makes them very promising materials to allow these technologies to fulfill their full potentials. Additionally, they could be very useful for other applications related to solar energy, for instance, thermoelectricity[4] and photocatalytic cells for water and air purification.[5]

Recently, there has been a major increase of interest in semiconductor nanowires.[6−8] When compared to semiconductor quantum dots, quantum wires satisfy the critical requirement for many practical applications; that is, the electron and hole conductivity should be retained for at least one dimension in order to inject or extract the carriers into or out from the nanostructures, while still being able to take advantage of novel physics phenomena associated with reduced dimensionality (e.g., quantum confinement, band structure engineering, reduced nonradiative recombination[9]

* Corresponding author. E-mail: yong_zhang@nrel.gov.
† Materials Science Center, National Renewable Energy Laboratory.
‡ Computational Research Division, Lawrence Berkeley National Laboratory.

10.1021/nl070174f CCC: $37.00
Published on Web 04/05/2007

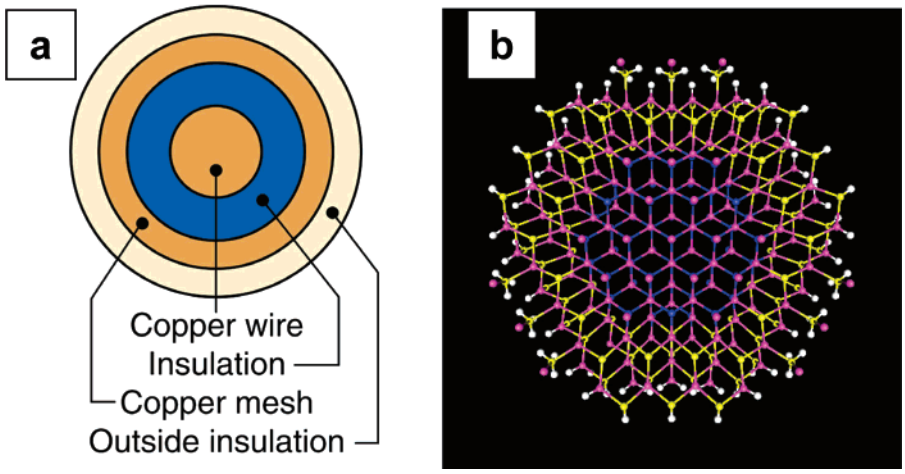

Figure 1. (a) Schematic of the cross section of a conventional coaxial cable. (b) Cross-section view of a "quantum coaxial cable", a GaN−GaP core−shell nanowire, with a GaN core, GaP shell, and hydrogen passivation shell (N, blue; P, yellow; Ga, magenta; H, white). The size of the wire is ∼4 nm. The horizontal axis is in the zinc-blende [$\bar{1}$10] direction, and the vertical is [$\bar{1}\bar{1}$2].

and carrier scattering[6]). A large variety of group IV, III−V, and II−VI nanowires have been grown or synthesized and investigated both experimentally and/or theoretically, including single component wires and core−shell wires. However, most efforts on core−shell wires have focused on structures consisting of core and shell materials with type I band alignments (e.g., GaP−Ga_2O_3, GaN/AlGaN, CdSe/ZnS),[10−12] where the shell provides either the conventional role (i.e., the quantum confinement effect to both electrons and holes in the core) or the role of a protective cladding to the core to reduce sensitivity to the environment. Core−shell wires with closely aligned band edges, e.g., ZnO−TiO_2, have been synthesized for the use in dye-sensitized solar cells,[13] and core−shell wires of Ge−Si with a small type II band alignment have been used for field effect transistors.[14] Although most core−shell wires reported are still relatively large (>100 nm), the sizes of Ge−Si wires have reached the quantum region (with a diameter around 15 nm). Nevertheless, there have been a few studies on type II core−shell quantum dots (e.g., CdTe−CdSe and CdSe−ZnTe or ZnTe−CdSe), in which the interesting effects of charge separation have indeed been observed.[15−18]

There are apparently a large number of electronic structure calculations for semiconductor quantum dots and single component nanowires (e.g., for various III−V and II−VI wires[19]), but far fewer on core−shell nanowires (e.g., for Si−Ge[20]). Because of the small type II alignment of the Si−Ge system,[21] the electronic structures of Si−Ge core−shell nanowires can be largely understood within the framework of quantum confinement.[20] We show that the physical properties change drastically for the core−shell wires involving components with large type II band alignments: for example, GaN−GaP(0.56/1.71), GaN−GaAs(0.2/2.18), ZnO−ZnTe(1.21/2.26), ZnO−ZnSe(1.0/1.53), and ZnO−ZnS(1.54/1.0),[22] where the numbers given in the parentheses are the energies (in eV) of the conduction band minimum (CBM) and valence band maximum (VBM) of the second component measured with respect to those of the CBM and VBM, respectively, of the first component. Figure 2 depicts the band

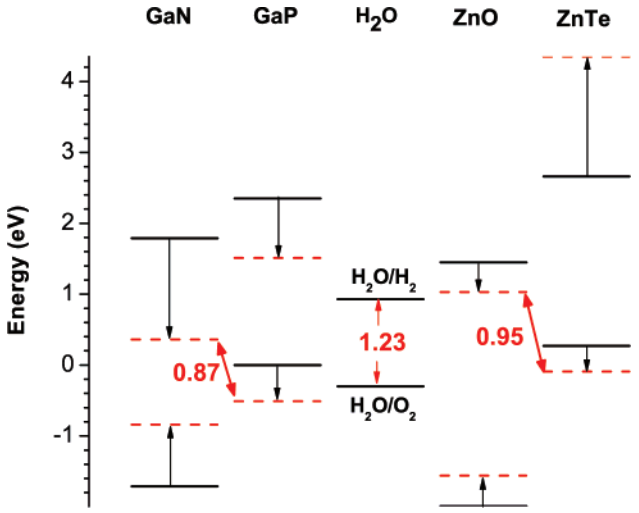

Figure 2. Energy diagrams of bulk semiconductors GaN, GaP, ZnO, and ZnTe and the chemical reaction potential energies of H_2O. Solid lines indicate the band edge energies (the conduction band minimum and valence band maximum) with natural lattice constants, dashed lines with average lattice constants between GaN and GaP or between ZnO and ZnTe.

diagrams for two prototype systems in their natural and average lattice constants. Such a type II combination has been found to result in a number of unusual effects in a seemingly unrelated field of semiconductor research, i.e., isoelectronic doping, because even an extremely small cluster of one component embedded in a bulk of the other component is capable of forming a bound state. For instance, a single N (O) atom has a bound state in bulk GaP (ZnTe),[23] which represents the smallest possible (type II) quantum dot.[24] The type II core−shell nanowires are expected to provide a band gap tunable range far exceeding that obtainable with the conventional approach of alloying the same two binaries. Although the upper limit will still be close to that of the larger band gap component, ∼3.4−3.5 eV for GaN and ZnO, the lower limit could be substantially lower than that of the lower band gap component. The lower limit

can be estimated to be $E_g^{min} = CBM_1 - VBM_2 + tr(\epsilon_1) D_{CB_1} - tr(\epsilon_2) D_{VB_2}$, where CBM_1 is the lower of CBM's and VBM_2 the higher of the VBM's of the two components, D_{CB_1} and D_{VB_2} are hydrostatic deformation potentials for the CBM_1 and VBM_2, respectively, and $tr(\epsilon)$ is the trace of the hydrostatic strain. Note that this serves only as a very rough estimate, because in the core−shell wire the atomic defomation is neither hydrostatic nor uniform. We define the composition of the core−shell wire to be $x = N_{core}/(N_{core} + N_{shell})$, where N_{core} and N_{shell} are, respectively, the total number of atoms in the core and shell. At $x = 0.5$, we have these rough estimates: E_g^{min} (GaN−GaP) = 0.87 eV and E_g^{min} (ZnO−ZnTe) = 0.95 eV, using Vegard's law for estimating lattice constants and calculated deformation potentials.[25] The exact band gap will be determined by the combined effects of quantum confinement, composition, lattice relaxation, and interface polarization. For instance, for a P-rich GaN−GaP wire, the actually calculated band gap could be lowered even to below 0.5 eV, reaching the spectral range appropriate for thermal photovoltaics where very few practical options are available.

To design a coaxial nanowire that meets the specific requirements for the intended application and understand quantitatively its electronic properties, we have performed first-principles pseudopotential density function calculations, within the local-density approximation (LDA), using a plane-wave code named PEtot.[26] Norm-conserving pseudopotentials are used. The results on prototype structures based on zinc-blende GaN and GaP (with either of them as the core) will be presented and discussed, although qualitatively similar results have also been obtained for wurtzite and II−VI materials (e.g., ZnO and ZnSe). The GaN−GaP or GaP−GaN core−shell nanowires are constructed with the wire axis along the zinc-blende[111] direction. The atomic positions in the structure are relaxed by a valence-force-field (VFF) method[27] that minimizes the elastic energy due to the lattice mismatch of the two components. The VFF parameters are derived from elastic constants of the relevant binaries (GaP, $\alpha = 46.2$ and $\beta = 10.7$; GaN, $\alpha = 85.0$ and $\beta = 15.9$). Although there is generally a strong lattice distortion after relaxation, due to the relatively large lattice mismatch, the 4-fold atomic coordination is retained for the structures explicitly calculated in this work. The wire surface is passivated by pseudohydrogen atoms[19] to shift the surface states far away from the fundamental band gap of the primary interest of this work. This practice mimics an optimized passivation that could be achieved experimentally.[28] For the-[111] nanowire, there are equal number of the cation and anion surface atoms with either one or two dangling bonds. The bond length between the pseudo-H and the surface atom is typically set to one-half of that in the bulk.[19] Although different core−shell structures have been calculated, we will illustrate the design principles primarily with the numerical results of one particular structure with 8 atomic shells in the core region or $N_{core} = 110$ atoms/period, 10 atomic shells in the shell region or $N_{shell} = 192$ atoms/period, and 90 pseudo-H atoms. The diameter of the core (determined by the outermost atomic shell) is $\sim 2\sqrt{13/6}a(x)$(≈15 Å for GaN−GaP), and of the core and shell $\sim 2\sqrt{13/2}a(x)$(≈26 Å for GaN−GaP), where $a(x)$ is the lattice constant determined by Vegard's law. Note that the core−shell wire does not have cylindrical symmetry, but is faceted with C_{3v} symmetry, as shown in Figure 1b, reflecting the atomistic nature in the nano region. The calculation is performed in a supercell approach using a hexagonal cell with the edges along $[\bar{1}10]$ and $[0\bar{1}1]$, respectively, and a sufficient cell size (such that the distance between the nearest atoms of the adjacent wires is >10 Å) to ensure the band gap energy is converged to within 10 meV. For the particular structure mentioned above, the length of the edge is $5\sqrt{2}a_{GaP}$. The Brillouin zone integration is performed using the Monkhost-Pack special k-points scheme with a mesh of $1 \times 1 \times 4$. A 35 Ry kinetic energy cutoff is used for the plane-wave expansion. The eigenvalues are converged to 10^{-4}−10^{-5} eV. The Ga pseudopotential is generated with a nonlocal core correction (i.e., the 3d states are not included in the valence electrons). After the electron charge density of the system is obtained by a total energy calculation, empirical corrections to the nonlocal pseudopotentials of Ga, P, and N atoms are introduced to correct the LDA errors in the bandgaps of the two binaries, as described in ref 29. The bandgaps at the X, L, and Γ points before (after) the corrections are for GaP $E_{gX} = 1.524$ (2.350) eV, $E_{gL} = 1.621$ (2.716) eV, and $E_{g\Gamma} = 1.757$ (2.887) eV, and for GaN, $E_{g\Gamma} = 1.888$ (3.301) eV, $E_{gX} = 3.292$ (4.676) eV, and $E_{gL} = 4.677$ (6.271) eV. The corrected values are typically within a few tens of millielectronvolts of the experimental values. Such corrections are particularly important for the core−shell structure, because the LDA errors are quite different for the two components. Using the same procedure, we have recently investigated small clusters of GaN embedded in GaP,[30] where the calculated binding energy of the single N impurity is found to agree with the experimental result to within 10 meV, despite the use of an approximate total charge density assembled by a charge patching scheme.[31]

Figure 3 shows the charge distributions (the squares of the wavefunctions) for the CBM and VBM in GaN−GaP and GaP−GaN core−shell wires for the structures described above. For the GaN−GaP wire, as shown in Figure 3a, the electron is largely localized in the GaN core, whereas the hole is confined to the GaP shell, although there is a small overlapping near the core−shell interface. The band gap of this GaN−GaP wire is 1.223 eV (compared to $E_g^{min} \sim -0.24$ eV). For the reversed GaP−GaN wire, as shown in Figure 3b, the electron is largely confined to the GaN shell, whereas the hole is now localized in the GaP core, which is the exact opposite of the former. The band gap of this GaP−GaN wire is 1.207 eV (compared to $E_g^{min} \sim 1.4$ eV), which turns out to be practically the same as the former, although such agreement is not always expected between the reversed structures. However, this does provide the leverage to select the structure based on the specific consideration of an intended application. The separation of the electron and hole bears a close similarity to that in a conventional coaxial cable, especially for the low-frequency signal, except that in a "quantum coaxial cable" the insulating spacer is not needed.

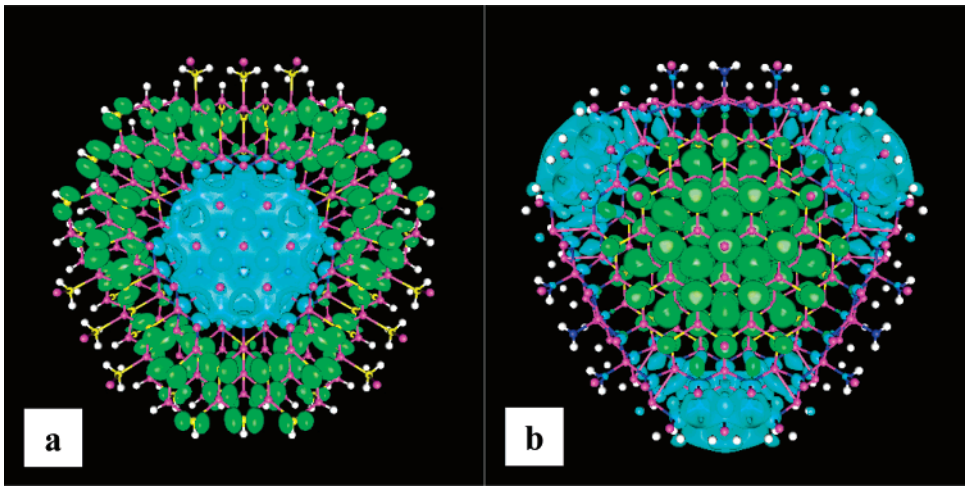

Figure 3. Cross-section views of charge distributions of the CBM electron state (cyan) and VBM hole state (green) in core−shell nanowires: (a) GaN(core)−GaP(shell); (b) GaP(core)−GaN(shell). The color codes for the atoms are the same as in Figure 1b.

The small residual electron−hole overlapping is expected to yield a significantly prolonged carrier lifetime, compared to that in a single-component nanowire, as has been demonstrated for core−shell quantum dots.[17] Concomitantly, it is the small overlapping that preserves finite absorption at the fundamental band gap, which has been utilized in the core−shell quantum dots for biomedical imaging.[16] The degree of overlapping is tunable by adjusting both the overall wire size $N = N_{core} + N_{shell}$ and the ratio N_{core}/N_{shell} to accommodate a particular application. For a GaN−GaP core−shell wire with a substantially larger GaP shell (N_{shell} = 888 atoms/period or outer diameter $\sim 2\sqrt{133/6}a(x) \approx 49$ Å) but the same size GaN core, we have used the charge-patching method[31] to get an estimate for its band gap, which yields a band gap of 0.588 eV. The actual band gap could very likely be below 0.5 eV, because this approximate approach does not adequately treat the interface polarization and, thus, tends to overestimate the band gap for the core−shell structure with a large lattice mismatch.

Next we examine the interesting behavior of higher subbands that are also practically important. For the GaN−GaP wire, the second conduction band at the Γ point (CB2Γ), at 0.616 eV above the CBM, is a doublet whose wavefunction remains localized in the core. Thus, the CBM and CB2Γ are states primarily derived from the GaN conduction band. The splitting can be understood as a result of crystal field splitting of the folded GaN conduction band states. The third conduction band at the Γ point (CB3Γ), at 0.740 eV above the CBM, is a singlet whose wavefunction has become more spread in the shell than in the core, which could be loosely viewed as derived from the GaP conduction band. This state is analogous to the LUMO (lowest unoccupied molecular orbit) of dye molecules that coat around a high band gap semiconductor in an intuitive picture of a dye-sensitized solar cell,[2,13] where the optical excitation from the HOMO (highest occupied molecular orbit) to the LUMO is generally considered to be responsible for generating electrons and holes. For the GaN−GaP core−shell wire, the corresponding transition energy of the "sensitizer", the GaP shell, will then be 1.961 eV, which is actually very similar to that of a typical dye used in a dye-sensitized solar cell. However, it eliminates the use of typically less stable organic molecules. Furthermore, the core−shell wire can shift the absorption threshold to as low as ∼1.22 eV of the fundamental band gap, thus enabling much more efficient collection of the solar spectrum. The subband levels are usually more closely spaced in the valence band, and their band edge states remain confined to the shell at least up to the fourth subband. In fact, there is a secondary band gap of 1.275 eV, corresponding to the transition from the double degenerate second valence band state at the Γ point (VB2Γ) to the CBM. And typically the dipole transition matrix element of VB2Γ → CBM is much stronger than that of VBM → CBM. The very effective electron and hole separation in this system, which is expected to remain so even at room temperature or higher, is obviously benefited from the large band edge energy mismatches between GaN and GaP. Figure 4 display cross-sectional views of the integrated charge distributions over the wire period for the first three subbands of both conduction and valence band. Reflecting the atomistic symmetry of the structure, the wavefunctions do not exhibit cylindrical symmetry.

Although the core−shell arrangement of GaN−GaP or ZnO−ZnSe is appropriate for a "semiconductor sensitized" solar cell, it is appropriate to adopt the reversed arrangement such as GaP−GaN for H_2 generation via photoelectrochemical water splitting for two considerations: (1) easier injecting electrons into the solution and (2) anti-corrosion. GaN would be an excellent material for the intended application if not for its band gap being too large to capture the major part of the solar spectrum.[32] GaPN alloy is an alternative material being actively researched, because N incorporation has been found to not only lower the band gap, but also improve the stability.[33] However, the VBM of GaPN remains ∼300 meV too high, and the stability is not satisfactory. In addition, an intrinsic limitation of the GaPN alloy is its poor carrier conductivity due to the formation of N cluster states.[34] A GaP−GaN core−shell wire can simultaneously overcome these major limitations. For the GaP−GaN wire, CB2Γ is also a doublet, located at 40 meV above the CBM and

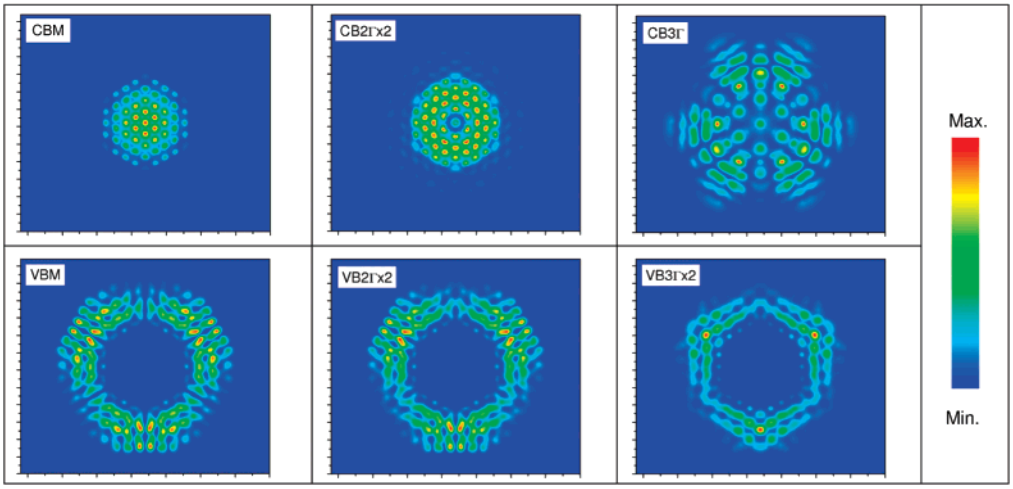

Figure 4. Cross-section views of integrated charge distributions over the wire period for a GaN−GaP core−shell nanowire. The scale of each frame is 7.70 nm (width) × 6.67 nm (height).

remaining in the shell region. The VB2Γ, a doublet, is at 0.354 eV below the VBM and strongly confined to the GaP core. The fundamental band gap of this prototype structure, 1.207 eV, is in fact very close to the energy needed for water splitting, 1.23 eV, although this could be a little too small in practice, so structural fine-tuning might be necessary. For instance, by increasing GaN shell to 264 atoms/period while keeping the same GaP core, the fundamental band gap will raise to 1.452 eV.

For application to the traditional solid state solar cell, one could envision adopting a somewhat simplified structure, that is, to have for instance GaN nanowires embedded in a GaP matrix. Our calculation (via the charge patching method) has indicated that the fundamental band gap of such an embedded structure, where the GaN regions behaves as an "anti-wire" for the hole, is comparable although somewhat smaller than that of the core−shell structure with the similar composition ratio. The general consideration here is to keep the fundamental band gap close to that corresponding to the optimized open-circuit voltage, but facilitate maximum electron−hole separation and, thus, minimize radiative recombination loss, and concurrently introduce a secondary nearby band gap that is higher than the fundamental band gap by a moderate value $>kT$ and with reasonable absorption strength. The proposed structure can do just that. For instance, for the GaN−GaP core−shell wire, the second band gap with reasonable absorption strength is appropriately at ∼50 meV higher than the first one. If successfully made, this system could offer a band gap tunable range from near-infrared to near-UV, yet without sacrificing the electronic conductivity that is found to be very poor when attempting to alloy GaP(As) with GaN.

We offer a few brief comments on implementing these structures in real devices. For the "semiconductor sensitized" solar cell, one could envision a device structure very similar to that of a dye-sensitized solar cell using ZnO nanowires.[35] For hydrogen generation via photoelectrochemical water splitting, a similar device structure may also be adopted. For the conventional solar cell, the material with embedded nanowires could simply replace the active layer in an existing structure. For all these applications, it is not necessary to have the core−shell nanowire doped. Even though for the hydrogen generation case, p-type doping is usually desirable for driving the electrons to the sureface, in the core−shell structure, the spontaneous charge separation has already produced such effect or an effective radial p−n junction. Nevertheless, doping the core−shell nanowire may provide further flexibility in the device design. All these materials (GaN, GaP, ZnO, ZnSe) are known to be easily made n-type, and the small gap materials are also easily made p-type. A quantitative understanding of the doping in such nanowires is of great interest and importance for future studies.

Besides those practical and important renewable energy applications discussed above, being a unusual type of quasi one-dimensional system, quantum coaxial wires are expected to open up new avenues for studying novel physics and material sciences in reduced dimensionality, including electronic conductivity, electron−hole correlation, spintronics, and ferroelectricity. Beyond the renewable energy applications, they could have numerous other exciting applications ranging from quantum computing to nanoelectronics.

Acknowledgment. We thank Dr. John Pern of NCPV for valuable discussions on photoelectrochemical water splitting and dye-sensitized solar cells. This work was supported by NREL LDRD, the U.S. DOE under Contract Nos. DE-AC36-99GO10337 to NREL and DE-AC03-76SF00098 to LBNL. This work used the computational resources of NERSC at LBNL.

Note Added after ASAP Publication. This paper was published ASAP on April 5, 2007. The color codes in the caption of Figure 3 were revised. The updated paper was reposted on April 25, 2007.

References

(1) Bak, T.; Nowotny, J.; Rekas, M.; Sorrell, C. C. *Int. J. Hydrogen Energy* **2002**, *27*, 991.
(2) Gratzel, M. *Nature (London)* **2001**, *414*, 338.
(3) Mascarenhas, A.; Zhang, Y.; Millunchick, J. M.; Twesten, R. D.; Jones, E. D. In *Future Generation Photovoltaic Technologies: Proceedings of the First NREL Conference (AIP Conference Proceedings No. 404), 1997*; McConnell, R. D., Ed.; The American Institute of Physics: New York, 1997; pp 303.

(4) Yang, R. G.; Chen, G.; Dresselhaus, M. S. *Nano Lett.* **2005**, *5*, 1111.
(5) Asahi, R.; Morikawa, T.; Ohwaki, T.; Aoki, K.; Taga, Y. *Science* **2001**, *293*, 269.
(6) Li, Y.; Qian, F.; Xiang, J.; Lieber, C. M. *Mater. Today* **2006**, *9*, 18.
(7) Thelander, C.; Agarwal, P.; Brongersma, S.; Eymery, J.; Feiner, L. F.; Forchel, A.; Scheffler, M.; Riess, W.; Ohlsson, B. J.; Gösele, U.; Samuelson, L. *Mater. Today* **2006**, *9*, 28.
(8) Pauzauskie, P. J.; Yang, P. D. *Mater. Today* **2006**, *9*, 36.
(9) Zhang, Y.; Sturge, M. D.; Kash, K.; van der Gaag, B. P.; Gozdz, A. S.; Florez, L. T.; Harbison, J. P. *Phys. Rev. B* **1995**, *51*, 13303.
(10) Kim, B.-K.; Kim, J.-J.; Lee, J.-O.; Kong, K.-j.; Seo, H. J.; Lee, C. J. *Phys. Rev. B* **2005**, *71*, 153313.
(11) Qian, F.; Li, Y.; Gradecak, S.; Wang, D. L.; Barrelet, C. J.; Lieber, C. M. *Nano Lett. (U.S.A.)* **2004**, *4*, 1975.
(12) Mokari, T.; Banin, U. *Chem. Mater.* **2003**, *15*, 3955.
(13) Law, M.; Greene, L. E.; Radenovic, A.; Kuykendall, T.; Liphardt, J.; Yang, P. D. *J. Phys. Chem. B* **2006**, *110*, 22652.
(14) Xiang, J.; Lu, W.; Hu, Y. J.; Wu, Y.; Yan, H.; Lieber, C. M. *Nature (London)* **2006**, *441*, 489.
(15) Hatami, F.; Grundmann, M.; Ledentsov, N. N.; Heinrichsdorff, F.; Heitz, R.; Bohrer, J.; Bimberg, D.; Ruvimov, S. S.; Werner, P.; Ustinov, V. M.; Kop'ev, P. S.; Alferov, Z. I. *Phys. Rev. B* **1998**, *57*, 4635.
(16) Kim, S.; Lim, Y. T.; Soltesz, E. G.; De Grand, A. M.; Lee, J.; Nakayama, A.; Parker, J. A.; Mihaljevic, T.; Laurence, R. G.; Dor, D. M.; Cohn, L. H.; Bawendi, M. G.; Frangioni, J. V. *Nat. Biotechnol.* **2004**, *22*, 93.
(17) Chen, C. Y.; Cheng, C. T.; Yu, J. K.; Pu, S. C.; Cheng, Y. M.; Chou, P. T.; Chou, Y. H.; Chiu, H. T. *J. Phys. Chem. B* **2004**, *108*, 10687.
(18) Xie, R. G.; Zhong, X. H.; Basche, T. *Adv. Mater.* **2005**, *17*, 2741.
(19) Li, J.; Wang, L.-W. *Phys. Rev. B* **2005**, *72*, 125325.
(20) Musin, R. N.; Wang, X.-Q. *Phys. Rev. B* **2005**, *71*, 155318.
(21) Schaffler, F. *Semicond. Sci. Technol.* **1997**, *12*, 1515.
(22) Wei, S.-H.; Zunger, A. *Appl. Phys. Lett.* **1998**, *72*, 2011.
(23) Cuthbert, J. D.; Thomas, D. G. *Phys. Rev.* **1967**, *154*, 763.
(24) Zhang, Y.; Ge, W. K. *J. Lumin.* **2000**, *85*, 247.
(25) Li, Y.-H.; Gong, X. G.; Wei, S.-H. *Phys. Rev. B* **2006**, *73*, 245206.
(26) Wang, L.-W. http://hpcrd.lbl.gov/∼linwang/PEtot/PEtot.html.
(27) Keating, P. *Phys. Rev.* **1966**, *145*, 637.
(28) Huang, X. Y.; Lindgren, E.; Chelikowsky, J. R. *Phys. Rev. B* **2005**, *71*, 165328.
(29) Wang, L. W. *Appl. Phys. Lett.* **2001**, *78*, 1565.
(30) Zhang, Y.; Mascarenhas, A.; Wang, L.-W. *Phys. Rev. B* **2006**, *74*, 041201(R).
(31) Wang, L. W. *Phys. Rev. Lett.* **2002**, *88*, 256402.
(32) Beach, J. D.; Collins, R. T.; Turner, J. A. *J. Electrochem. Soc.* **2003**, *150*, A899.
(33) Deutsch, T. G.; Koval, C. A.; Turner, J. A. *J. Phys. Chem. B* **2006**, *110*, 25297.
(34) Zhang, Y.; Fluegel, B.; Mascarenhas, A.; Xin, H. P.; Tu, C. W. *Phys. Rev. B* **2000**, *62*, 4493.
(35) Law, M.; Greene, L. E.; Johnson, J. C.; Saykally, R.; Yang, P. D. *Nat. Mater.* **2005**, *4*, 455.

NL070174F